Hindawi Publishing Corporation
International Journal of Optics
Volume 2012, Article ID 902849, 12 pages
doi:10.1155/2012/902849

Research Article

Bottom-Up Abstract Modelling of Optical Networks-on-Chip: From Physical to Architectural Layer

Alberto Parini,[1,2] Luca Ramini,[2] Fabio Lanzoni,[2] Gaetano Bellanca,[2] and Davide Bertozzi[2]

[1] *Laboratory for Micro and Submicro Enabling Technologies of the Emilia-Romagna Region (MIST E-R), Via P. Gobetti 101, 40129 Bologna, Italy*
[2] *Department of Engineering, University of Ferrara, Via Saragat 1, 44122 Ferrara, Italy*

Correspondence should be addressed to Alberto Parini, alberto.parini@unife.it

Received 14 August 2012; Accepted 19 October 2012

Academic Editor: Giovanna Calò

This work presents a bottom-up abstraction procedure based on the design-flow FDTD + SystemC suitable for the modelling of optical Networks-on-Chip. In this procedure, a complex network is decomposed into elementary switching elements whose input-output behavior is described by means of scattering parameters models. The parameters of each elementary block are then determined through 2D-FDTD simulation, and the resulting analytical models are exported within functional blocks in SystemC environment. The inherent modularity and scalability of the *S*-matrix formalism are preserved inside SystemC, thus allowing the incremental composition and successive characterization of complex topologies typically out of reach for full-vectorial electromagnetic simulators. The consistency of the outlined approach is verified, in the first instance, by performing a SystemC analysis of a four-input, four-output ports switch and making a comparison with the results of 2D-FDTD simulations of the same device. Finally, a further complex network encompassing 160 microrings is investigated, the losses over each routing path are calculated, and the minimum amount of power needed to guarantee an assigned BER is determined. This work is a basic step in the direction of an automatic technology-aware network-level simulation framework capable of assembling complex optical switching fabrics, while at the same time assessing the practical feasibility and effectiveness at the physical/technological level.

1. Introduction

Chip multicore architectures currently represent the state of the art in the design of high performance very large scale integration (VLSI) systems. In accordance with this architectural paradigm, several processing units are physically realized on the same silicon die and share the execution of the instructions with a high degree of parallelism. For the next generation of digital systems, the International Technology Roadmap for Semiconductors (ITRS) expects the integration on the same substrate of hundreds of computational cores [1]. To assure a fast and reliable communication over a network with such a complexity, a traditional bus-based solution is no more conceivable. From a technological point of view, a straightforward and alternative way to implement the communication among the cores is to create, at the chip level, a network-based link system (Network-on-Chip (NoC)) [2]. However in an NoC implemented with electrical links (electronic Networks-on-Chip (ENoC)), as the number of interconnected cores increases, the constraints in terms of power dissipation and required bandwidth grow exponentially, thus imposing soon unrealistic conditions for practical achievements [3]. To overcome these problems, the realization of optical-based interconnections among cores (optical Network-on-Chip (ONoC)) appears as a promising solution, both for power consumption and allowable bandwidth [4, 5].

The predominance of optics with respect to electronics has been clearly proved for long and extra-long haul telecommunication systems, with the replacement of copper cables with single-mode optical fibers. At present days, the aim is to introduce photonics over extra short links, at chip-to-chip or even on-chip levels. The capability to exploit optical devices in a network of extrasmall dimensional scale, relies upon the last achievements of integrated photonics and, in particular, of SOI (Silicon-on-Insulator) technology

(basically for its full compatibility with CMOS logics) [6]. Many research units worldwide are working in this direction [7] and, furthermore, on the integration of silicon with III-V materials (also to include sources [8] and detectors [9] and to exploit nonlinearities [10]). By following the last trends of 3D integration in digital systems, it is possible to conceive a vertical stack with a top layer reserved to the optical communication network, superposed to silicon layers incorporating memory and processing units.

A complex ONoC can be considered as the composition of several elementary building-blocks named photonic switching elements (PSEs). Each PSE is an atomic optical fabric able to route a signal from one input towards a specific output (1×2 PSE), or from two inputs towards two output ports (2×2 PSE). The 1×2 PSEs are typically used to derive higher-order switching structures, as illustrated with a simple example in Figure 1. Another example of this approach is reported in [11], where a spatially nonblocking 4×4 router is demonstrated. A similar structure, but with a different layout, is used in [12] to provide non-blocking and low-loss switching. In [13], instead, 2×2 PSEs are used to structure the so-called 4×4 GWOR (generic wavelength-routed optical router). In a similar fashion, [14] proposes a lambda-Router, a multistage network, where the basic cells are 2×2 PSEs with parallel access waveguides.

For the design and the optimization of such complex optical networks, the availability of efficient and reliable tools is fundamental. These tools should combine the flexibility and the versatility needed to analyze the high level architecture layers, with the capability to represent accurately the basic communication parameters such as, for example, attenuation and bandwidth, which are strictly linked with the physics of these devices. Indeed, taking into account these parameters also at higher level of abstraction (by means of what we identify here as technological annotation) is fundamental to explore how constraints imposed by the technological aspects can affect the implementation of an optical interconnection network for chip-level integrated systems.

Among the available tools, PhoenixSim [15] is certainly a relevant simulation environment structured in OMNET++. This tool is capable of assessing the performance of multiprocessor hybrid systems, integrating electronic and optical networks on the same platform. The key feature of PhoenixSim lies in the modelling parameters, such as: propagation delay, insertion loss, occupation area on the chip, and energy consumption. All these figures of merit are obtained on hardwired precharacterized values for given wavelengths. For this purpose, PhoenixSim does not use any analytical model for insertion loss analysis.

Although with PhoenixSim it is possible to explore optical on chip networks using a physical layer analysis, it lacks compliance with industry-standard hardware modelling languages and methodologies; for this reason, PhoenixSim was recently augmented with a SystemC wrapper. On the other hand, this procedure is onerous in terms of computation time. We instead aim at modeling optical NoCs leveraging on a plain SystemC modeling style. SystemC is an open-source system-level design language based on C++, which extends the modelling capabilities of traditional hardware description languages (HDLs) to higher levels of abstraction. SystemC is particularly suitable for the analysis of electronic NoCs and, with some appropriate extensions, can be used also for optical NoCs.

The first example of modeling framework in SystemC is presented in [16]. Here, separate channels are used to model wavelength and power information of optical signals. In [17], a new SystemC class is created to manage analog signals transmitted between modules which access communication channels through the typical constructs of abstract simulation (e.g., FIFO constructs of untimed functional simulation). Above all, the key issue of technology awareness is solved by invoking the Matlab *Symbolic Toolbox* for elaborating *S*-Matrices. In particular, the computation time of all the *S*-Matrices of each slice of a typical wavelength routed 4×4 optical crossbar is about 30 seconds on a 2.4 GHz Pentium 4.

With respect to this work, we aim at reusing the existing port-interface-channel constructs of SystemC, thus making the top-level view of an optical NoC looks like the same of an electronic NoC; the difference lies just in module implementations and in the data types exchanged through the predefined SystemC channels. Moreover, we leverage on the RTL (register-transfer level) modeling style for the sake of accuracy. We do not build a new SystemC class to manage analog signals in the network but, in contrast, we exploit the user-defined data type, and then we describe the optical information on three different fields such as logic value, wavelength, and signal amplitude.

The key challenge of our SystemC modeling framework lies in the integrating technology annotations in the abstract model to preserve a valuable degree of technology awareness while limiting repercussion in simulation time. Unlike [17], this work provides validation results of developed analytical models with respect to FDTD simulations. By doing so, in the first instance, the photonic elements composing the optical links are described at the phenomenological level through a set of analytical models of black-box type, whose parameters are determined through measurements or simulations. Basic optical switching components are then modelled in SystemC through a module that embeds both the functional behavior of the component as well as its nonfunctional information (i.e., technology annotations). This allows the exploration of different topologies for the ONoC, without losing the awareness of the fundamental physical constraints imposed by the optical devices used to compose the optical layer of the network. The basics of the proposed approach are described in the next sections; then, this technique is applied to analyze a 4×4 switch. Comparisons of SystemC results with the ones obtained through electromagnetic simulation of the overall device by finite difference in the time domain (FDTD) [18] are used to validate the implemented model. A more complex structure (4×4 square root) [19], realized by compositions of these 4×4 switches, is therefore investigated, and its insertion loss and the optical power required by the laser source to meet a fixed detector sensitivity are quantified. Finally, conclusions are drawn.

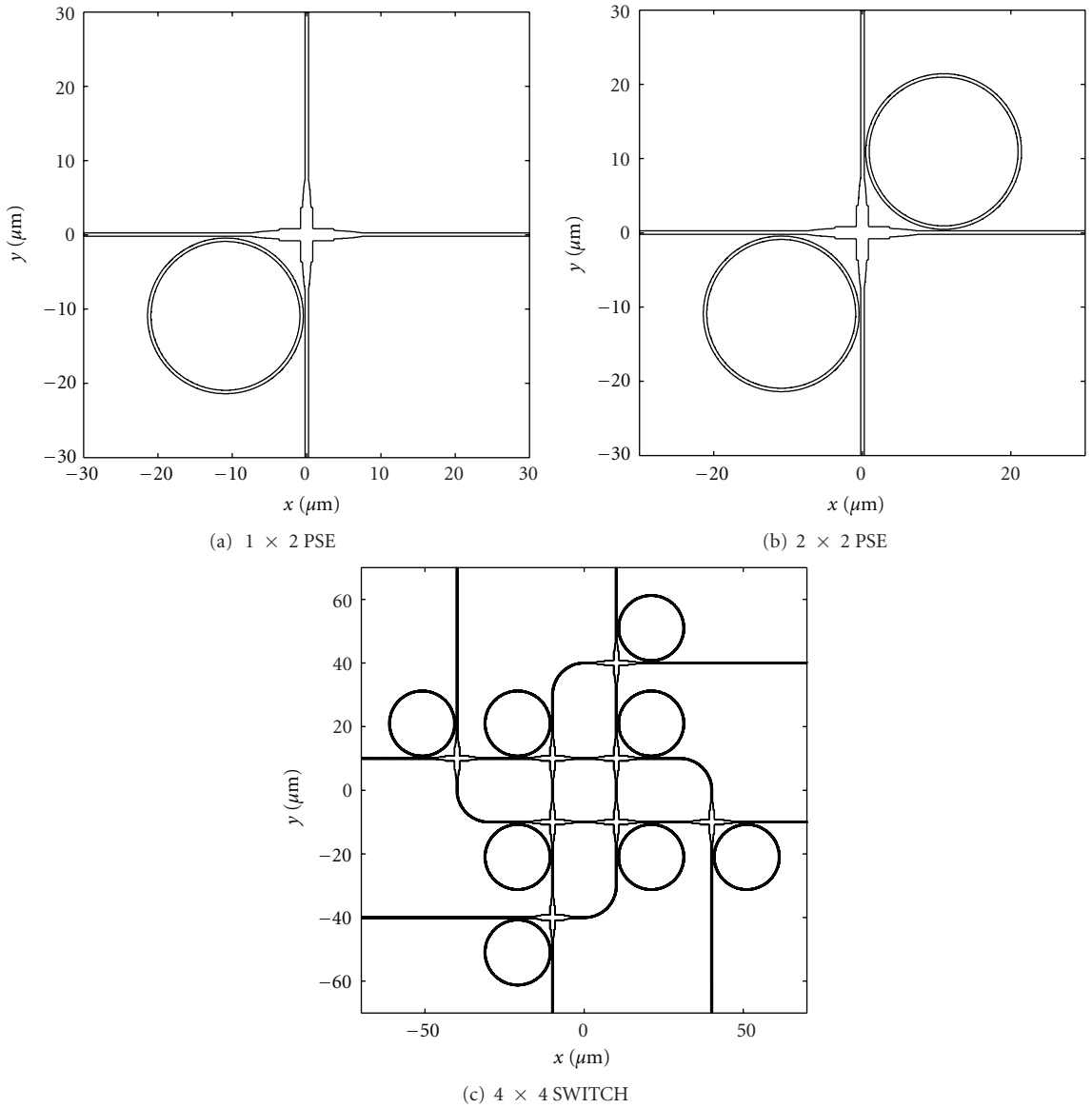

Figure 1: Sketch of a microring-based (a) 1 × 2 PSE, (b) 2 × 2 PSE, and (c) 4 × 4 optical switch. As one can observe, complex structures are obtained by compositions of the elementary building blocks.

2. Technology-Aware SystemC Simulation of Optical Networks-on-Chip

As previously stated, the architectural design of an optical Network-on-Chip must be performed with a simulation tool able to meet multiple requirements such as efficient network-level simulation, support for technology annotations, and compliance with the industrial standards for the design of electronic parts. The SystemC environment offers the necessary features to become the "state of the art" simulation tool in the system level design of optical Networks-on-Chip. More specifically, the key reasons that make SystemC the most effective choice are as follows.

(i) SystemC is an object-oriented C++ class library that offers a high level of modularity and flexibility. In particular, the base constructs can be custom-tailored to fulfill specific modelling requirements.

(ii) The communication semantics inside SystemC are based on a very flexible set of interface method calls. Consequently, the peculiar and distinctive features of optical links can be captured by leveraging on the preexisting communication constructs of SystemC.

(iii) SystemC can easily span over a wide range of abstractions layers, from register-transfer level (RTL) up to untimed functional (UF), thus allowing both high level of accuracy or reduction of the computation time.

Therefore, SystemC may serve as a unified description language able to overcome the limitations of cosimulation

approaches. It can provide local and global optimizations, allowing an easier exploration of the whole design space of ONoCs.

The bottom-up abstraction procedure, leading from the physical models up to their corresponding SystemC modules, can be summarized in the following steps.

(1) Description of the input-output relations of each functional component of the optical network (waveguides, bendings, and ring resonators) in analytical form, by means of the scattering parameters formalism.

(2) Electromagnetic simulation (or experimental characterization) of the elementary functional components to derive the input-output responses to be reproduced by the analytical models. This step must be repeated each time a modification of the physical parameters within the PSEs (waveguide sizes, gaps between rings and waveguides, ring radii, etc.) is introduced. To extend the flexibility of the modeling tool, a physical layer library (PLL) could be prepared to support the standard industrial technologies of the worldwide leading silicon foundries.

(3) Backannotation of the analytical models in SystemC, and validation with respect to the numerical or experimental data across the entire optical spectrum.

(4) Modular composition and modelling, inside the SystemC environment, of higher-order routing structures. By doing so, any component of the physical layer library must be abstracted into SystemC modules, thus expanding our SystemC photonics library (SPL). In this way, any physical change will be imported within our simulator, and network level analysis will be upgraded.

(5) Insertion-loss assessment of optical network topologies, and then evaluation of the minimum optical power that the laser sources should provide to enable correct detection of the optical data stream at the photodetectors.

To demonstrate the effectiveness of the proposed approach, a complex 4×4 square root topology will be investigated. The analytical model of this network will be obtained by composition of the scattering matrices (S-matrices) of the different elementary building blocks, whose parameters will be deduced through FDTD simulations. This procedure is detailed in the next sections.

3. S-Parameters Modelling of a 1×2 PSE

As mentioned in the introduction, the most simple PSE is a structure with one input and two possible output ports (1×2 PSE). Without loss of generality, in this work we refer to microring-based 1×2 PSE. To realize this component, other technological solutions are possible [20]. In all cases, however, the compositional approach proposed in this work can be easily applied for investigations.

In the case of ring-based ONoCs, the 1×2 PSE can be implemented via a microring resonator cascaded to a crossing between two orthogonal waveguides (see Figure 2). The device is active if the resonances of the microring can be dynamically adjusted via some thermal or charge-injection-based effects; otherwise, the device is passive, and the microring resonances are fixed and defined a priori. In the passive configuration, however, a slow thermal mechanism can be envisaged for fine tuning of the resonances in the final setup of the device.

To enable the bottom-up abstraction procedure outlined in the previous section, the optical behavior of the elementary 1×2 PSE is first described by means of an analytical model that takes the form of a finite set of linear equations.

In the first part of this section, the optical propagation in a microring resonator and in a crossing between two waveguides is described with the well-known formalism of the scattering matrices; in the second part, the S-matrices of microring and crossing are cascaded to obtain the comprehensive model for the passive 1×2 PSE. Then, the parameters of the S-matrix are optimized to match the transmission properties obtained through FDTD simulations.

A microring resonator and a crossing between two waveguides (network α and β in Figure 2) can be both represented as four-ports devices; consequently, the relations between the input and output signals at their ports can be modeled by means of 4×4 scattering matrices, whose coefficients depend on a finite set of parameters (optical lengths, coupling coefficients, and transmission efficiency). The resulting s-matrices are symmetrical because the networks under consideration are reciprocal. Without loss of generality, the gaps between the two waveguides and the ring are supposed to be equal and represented with the same power coupling coefficient K. Moreover, microring and waveguides are assumed to be dispersionless; thus, the effective index and the group index coincide; the propagation losses are also neglected. Dispersion effects, losses, or a coupling asymmetry between the waveguides and the ring can be easily taken into account in the model [21].

Under these assumptions, the S-parameters of the microring resonator (network α in Figure 2) read as

$$
\begin{aligned}
s_{12} = s_{21} &= \frac{-t^2 e^{-j(2\pi/\lambda)L_R a}}{1 - r^2 e^{-j(2\pi/\lambda)L_R}} e^{-j(\pi/\lambda)(L_{13}+L_{24})}, \\
s_{13} = s_{31} &= \frac{r - re^{-j(2\pi/\lambda)L_R}}{1 - r^2 e^{-j(2\pi/\lambda)L_R}} e^{-j(2\pi/\lambda)(L_{13})}, \\
s_{24} = s_{42} &= \frac{r - re^{-j(2\pi/\lambda)L_R}}{1 - r^2 e^{-j(2\pi/\lambda)L_R}} e^{-j(2\pi/\lambda)(L_{24})}, \\
s_{34} = s_{43} &= \frac{-t^2 e^{-j(2\pi/\lambda)L_R(1-a)}}{1 - r^2 e^{-j(2\pi/\lambda)L_R}} e^{-j(\pi/\lambda)(L_{13}+L_{24})},
\end{aligned}
\tag{1}
$$

where $r = \sqrt{1-K}$, $t = \sqrt{K}$, L_R is the optical length of the ring, and L_{13} and L_{24} are the optical lengths of the two access waveguides. The parameter $a = \theta/2\pi$ defines the relative angle between the two straight waveguides. The usual configuration with parallel waveguides corresponds to a value of $\theta = \pi (a = 0.5)$, while the configuration in Figure 2(a), where the relative angle between the waveguide is $\theta = \pi/2$, corresponds to $a = 0.25$. To further simplify,

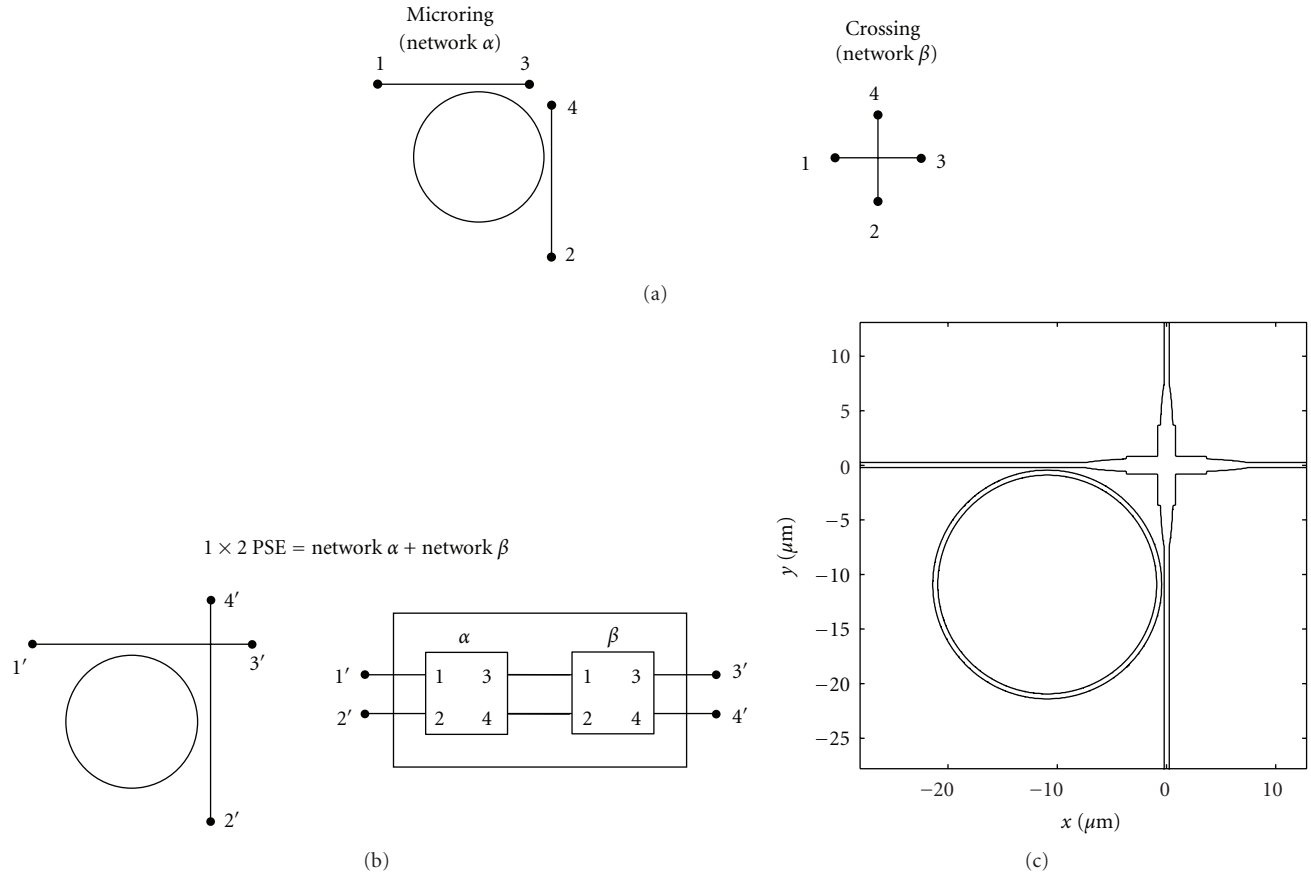

FIGURE 2: ((a)-left) Sketch of a microring resonator with orthogonal access waveguides. ((a)-right) Sketch of an orthogonal planar crossing. (b) The 1 × 2 PSE can be considered as the cascading of the microring α with the crossing β. If the wavelength of the optical carrier signal is resonant with the microring, the data stream on the Port 1′ is routed toward Port 2′; if the optical signal is not resonant, the data stream is routed to Port 3′. Dually, a signal coming from Port 4′ is routed to Port 3′ if resonant, while continuing to Port 2′ if out of resonance. The device is bidirectional, that is, each of the ports can act as input or output, but not simultaneously. (c) Representation of the PSE as it appears when discretized inside the 2D-FDTD code; in this case, the transmission at the intersection between the waveguides is optimized using an MMI-based crossing.

the back reflections are not included in the model ($s_{11} = s_{22} = s_{33} = s_{44} = 0$) and the cross-scattering coefficients are assumed to be negligible ($s_{14} = s_{41} = s_{23} = s_{32} = 0$). The scattering parameters can be finally cast in a matrix form that reflects the topology of the of the structure:

$$S_{\text{RING}} = \begin{bmatrix} 0 & s_{12} & s_{13} & 0 \\ s_{21} & 0 & 0 & s_{24} \\ s_{31} & 0 & 0 & s_{34} \\ 0 & s_{42} & s_{43} & 0 \end{bmatrix}. \tag{2}$$

A planar crossing between two waveguides, as the one presented in Figure 2 (network β), can be analogously described with a scattering matrix that takes the following form:

$$S_{\text{CROSS}} = \begin{bmatrix} 0 & 0 & s_{13} & 0 \\ 0 & 0 & 0 & s_{24} \\ s_{31} & 0 & 0 & 0 \\ 0 & s_{42} & 0 & 0 \end{bmatrix}, \tag{3}$$

where the coefficients $s_{13} = s_{31} = s_{24} = s_{42} = \sqrt{\eta}$ model the power transmission efficiency of the paths between Ports 1↔3 and between Ports 2↔4. High transmission efficiencies ($\eta \cong 1$) with crosstalk effects almost suppressed can be reached using elliptically-tapered intersections [22], or with a further optimized solution relying on multimode interference (MMI) structures [23].

Due to the fact that the 1 × 2 PSE can be considered as a cascade connection between networks α and β, as shown in Figure 2(b), the S-parameters matrix of the resulting network can be derived from the ones of the two connected blocks with some straightforward matrix manipulations [24]. Considering the s-parameters matrices of the two circuits, S_α and S_β,

$$S_\alpha = \begin{bmatrix} s_{11}^\alpha & s_{12}^\alpha & s_{13}^\alpha & s_{14}^\alpha \\ s_{21}^\alpha & s_{22}^\alpha & s_{23}^\alpha & s_{24}^\alpha \\ s_{31}^\alpha & s_{32}^\alpha & s_{33}^\alpha & s_{34}^\alpha \\ s_{41}^\alpha & s_{42}^\alpha & s_{43}^\alpha & s_{44}^\alpha \end{bmatrix},$$

$$S_\beta = \begin{bmatrix} s_{11}^\beta & s_{12}^\beta & s_{13}^\beta & s_{14}^\beta \\ s_{21}^\beta & s_{22}^\beta & s_{23}^\beta & s_{24}^\beta \\ s_{31}^\beta & s_{32}^\beta & s_{33}^\beta & s_{34}^\beta \\ s_{41}^\beta & s_{42}^\beta & s_{43}^\beta & s_{44}^\beta \end{bmatrix}. \tag{4}$$

The first step in order to compute the S-parameter matrix $S_{(\alpha+\beta)}$ of the resulting cascaded network is to partition both S_α and S_β into four sections. For network α, one can write

$$S_1 = \begin{bmatrix} s_{33}^\alpha & s_{34}^\alpha \\ s_{43}^\alpha & s_{44}^\alpha \end{bmatrix}, \quad S_2 = \begin{bmatrix} s_{13}^\alpha & s_{14}^\alpha \\ s_{23}^\alpha & s_{24}^\alpha \end{bmatrix},$$
$$S_3 = \begin{bmatrix} s_{31}^\alpha & s_{32}^\alpha \\ s_{41}^\alpha & s_{42}^\alpha \end{bmatrix}, \quad S_4 = \begin{bmatrix} s_{11}^\alpha & s_{12}^\alpha \\ s_{21}^\alpha & s_{22}^\alpha \end{bmatrix}, \tag{5}$$

whereas for network β, it holds:

$$S_5 = \begin{bmatrix} s_{11}^\beta & s_{12}^\beta \\ s_{21}^\alpha & s_{22}^\alpha \end{bmatrix}, \quad S_6 = \begin{bmatrix} s_{13}^\beta & s_{14}^\beta \\ s_{23}^\alpha & s_{24}^\alpha \end{bmatrix},$$
$$S_7 = \begin{bmatrix} s_{31}^\beta & s_{32}^\beta \\ s_{41}^\alpha & s_{42}^\alpha \end{bmatrix}, \quad S_8 = \begin{bmatrix} s_{33}^\beta & s_{34}^\beta \\ s_{43}^\beta & s_{44}^\beta \end{bmatrix}. \tag{6}$$

The eight submatrices, from S_1 to S_8, are then combined to obtain the partitions of $S_{(\alpha+\beta)}$:

$$\begin{aligned} S_I &= S_3 S_5 (I - S_1 S_5)^{-1} S_2 + S_4, \\ S_{II} &= S_3 S_5 (I - S_1 S_5)^{-1} S_1 S_6 + S_3 S_6, \\ S_{III} &= S_7 (I - S_1 S_5)^{-1} S_2, \\ S_{IV} &= S_7 (I - S_1 S_5)^{-1} S_1 S_6 + S_8, \end{aligned} \tag{7}$$

where I is the identity matrix of order two.

$S_{(\alpha+\beta)}$ reads finally as

$$S_{(\alpha+\beta)} = \begin{bmatrix} S_I & S_{II} \\ S_{III} & S_{IV} \end{bmatrix}, \tag{8}$$

and the relations between the input and output optical signals at the four ports are expressed by

$$\begin{bmatrix} O_{1'} \\ O_{2'} \\ O_{3'} \\ O_{4'} \end{bmatrix} = S_{(\alpha+\beta)} \times \begin{bmatrix} I_{1'} \\ I_{2'} \\ I_{3'} \\ I_{4'} \end{bmatrix}. \tag{9}$$

The coefficients of $S_{(\alpha+\beta)}$ must now be tuned in order to guarantee a minimum mismatch between the analytical and the numerical input-output responses (or the experimental measures, if available). To do so, we consider these responses as vectors depending on the wavelength, and we introduce an error parameter ε defined as the Euclidean norm of the difference between them. By spanning iteratively the values of the governing parameters (optical lengths of the rings, coupling factors, etc.) over searching intervals suitably defined as a function of geometry and materials of the structure, it is possible to find a minimum value for the error ε; this minimum corresponds to the best set of parameters for the given PSE.

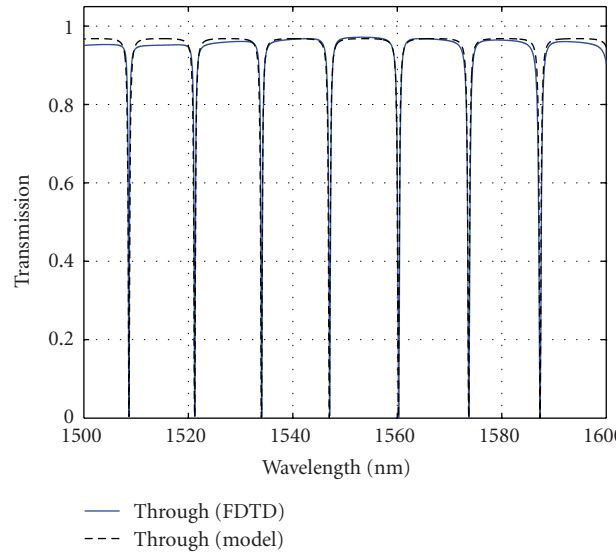

Figure 3: Comparisons between the spectral response of the Through Path (Port 1′ to Port 3′) of the passive 1 × 2 PSE, calculated via 2D-FDTD and by means of the s-matrix model.

In this paper, a simulation approach has been used, and the 1 × 2 PSE has been characterized through 2D-FDTD. A wide-band excitation signal in the wavelength range of 1500 nm–1600 nm has been applied to Port 1′ (see Figure 2) to evaluate the on-resonance (1′ → 2′) and off-resonance (1′ → 3′) spectral responses of the device. Figures 3 and 4 compare the results of the FDTD simulation (solid lines) with the ones of the s-parameters-based analytical model (dashed lines), once applied the optimized fitting procedure. The blue lines refer to the path between the Ports 1′ and 3′ (Through), whereas red lines refer to the path between Ports 1′ and 2′ (Drop). The physical and geometrical parameters of the tested PSE are internal radius of the ring $R = 10\,\mu$m, ring and waveguides width $w = 450$ nm, effective index of ring and waveguides $n_{\text{eff}} = 2.3561$, and physical gap $g = 300$ nm corresponding to a coupling coefficient $K = 0.0838$. The MMI-based crossing considered in this PSE provides a transmission efficiency $\eta = 0.975$.

4. SystemC Modelling of a 4 × 4 Optical Switch

The integration inside SystemC of the s-parameters model for the elementary 1 × 2 PSE allows the modular composition and characterization of higher-order routing structures. The first composite device under test, whose scheme is illustrated in Figure 5, is an optical switch with four input and four output ports, located along the cardinal points: North, East, South, and West. Such a structure is realized with eight elementary 1 × 2 PSEs, arranged in a matrix layout. This switch, with respect to other topologies proposed in

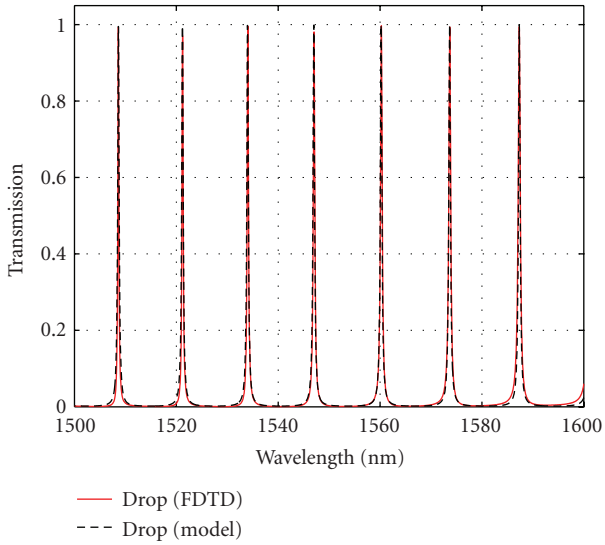

Figure 4: Comparisons between the spectral response of the Drop Path (Port 1′ to Port 2′) of the passive 1 × 2 PSE, calculated via 2D-FDTD and by means of the *s*-matrix model.

Table 1: Available routing paths inside the 4 × 4 optical switch.

Input port	On-resonance output port	Off-resonance output port
West	South	North
South	East	West
East	North	South
North	West	East

the literature [25], contains a limited number of waveguide crossings, thus keeping the overall propagation losses at an acceptable level for a practical realization.

In order to verify the correctness of the proposed compositional approach, the 4 × 4 optical switch (4 × 4 SW) has been first simulated with 2D-FDTD; then, the spectral response obtained from the numerical data has been compared with the one calculated with the SystemC analysis. By considering the 4 × 4 SW realized with eight 1 × 2 PSEs with ring radius of 10 μm (as the one previously analyzed in Section 2), the whole footprint of the structure is about 140 μm × 140 μm. Consequently, the FDTD simulation takes more than 72 hours on a parallel cluster of 10 processors Intel Xeon E5520. Due to the burden of the computational domain, the 4 × 4 SW is, on the available cluster, the upper bound for an FDTD electromagnetic simulation, and it represents the top benchmark for testing the reliability of the compositional abstraction procedure. On the contrary, the SystemC modelling requires only 0.001 seconds per wavelength to perform the analysis of a single considered optical path.

As illustrated in Figure 5(a), each 1 × 2 PSE is connected with other ones by means of specific physical links. However, depending on the wavelength of the signal respect to the resonance of each router, different logical paths must be considered for each connection between the input and the output ports. To describe the overall behavior of the network, SystemC should then model all these logical paths, taking into account all their relevant features.

To enable this functionality, we utilize a predefined standard communication channel of SystemC (i.e., sc-signal) with a new user-defined data type. This allows to replicate the relevant features of an optical link such as logic value (transmission of logical value "0" or "1"), optical wavelength, and signal amplitude. The optical wavelength is used by the router model to implement the routing functionality; the signal amplitude, on the contrary, is considered to take into account the technological awareness (such as insertion-loss on the direct path and cross-talk determined by spurious power addressed to other ports). To allow the computation of the optical power budget of each link, backannotation from FDTD to SystemC of losses in waveguides, bending, and crossing is therefore mandatory.

Figure 6 shows the transmission characteristic of the 4 × 4 optical switch when a signal is injected in the I-WEST port and collected at the O-NORTH port (Through Path). The PSEs involved in this communication are PSE-1, PSE-2, PSE-4, and PSE-5; the data stream is routed through this path if the wavelength of the carrier is not in resonance with the microrings (see Table 1). The solid blue line refers to the result of the FDTD simulation, while the black dotted line is the SystemC modelling; as illustrated by the figure, the SystemC approach fits perfectly the resonances and the global level of losses for the considered path. In a similar way, the transmission characteristic between the I-WEST port and the O-SOUTH port (Drop Path) is presented in Figure 7. Here, the signal is routed for wavelengths corresponding to the resonances of PSE-1. It must be noted that since this topology is symmetrical under step rotations of 90 degrees, the transmission curves are the same injecting the signal from all other inputs (South, East, and North).

Thanks to the accuracy of the technology annotations in SystemC, our framework gains control over both the resonant wavelengths of switching components and the signal amplitudes in optical paths. As a consequence, the comparative analysis of wavelength-routed versus space-routed optical NoCs, or the assessment of signal-to-noise ratio (SNR) at optical receivers, becomes feasible. In fact, such tasks require the knowledge of both the network behavior and of key implementation details and physical insights.

The accuracy of the SystemC-based modelling has been further analytically tested by evaluating two different quantities: the average error on the entire spectrum of the signal (SE) and the error on the peaks (PE). The former SE measures the mean squared error between the FDTD and SystemC spectral responses, and it has been calculated across the wavelength range from 1500 nm to 1600 nm by using the following expression:

$$\mathrm{SE} = \frac{\sum_{i=1}^{n} \left[T_{\mathrm{FDTD}}(\lambda_i) - T_{\mathrm{SysC}}(\lambda_i) \right]^2}{n} * 100. \tag{10}$$

Here, $T_{\mathrm{FDTD}}(\lambda_i)$ and $T_{\mathrm{SysC}}(\lambda_i)$ are the transmissions at the wavelength λ_i calculated by means of FDTD and SystemC,

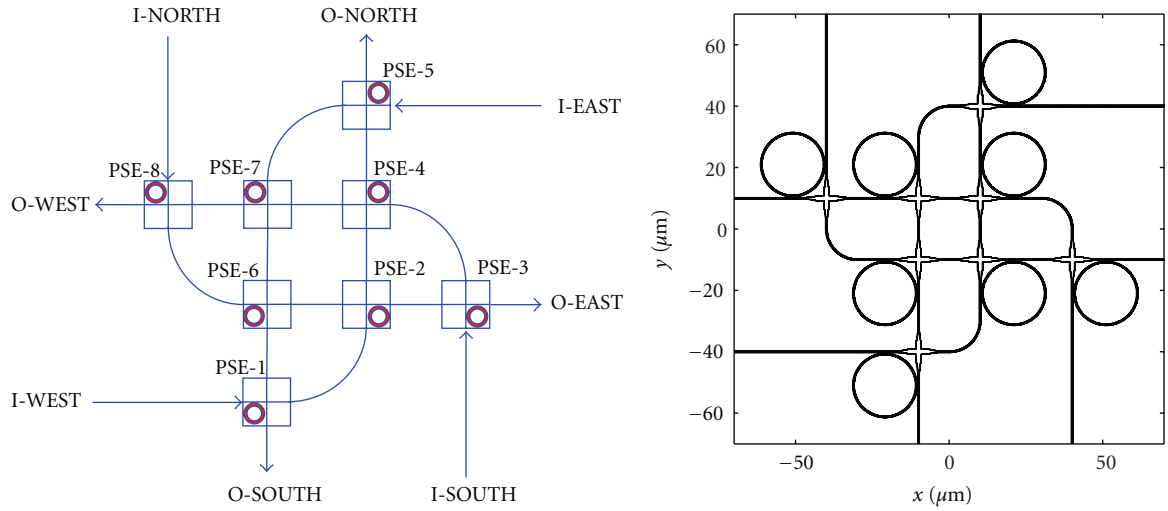

FIGURE 5: (a) Topological scheme of the 4 × 4 optical switch showing the interconnections between the eight PSEs. (b) FDTD representation of the real device; the computational domain is discretized over a grid with step $dx = dy = 1/30\,\mu$m.

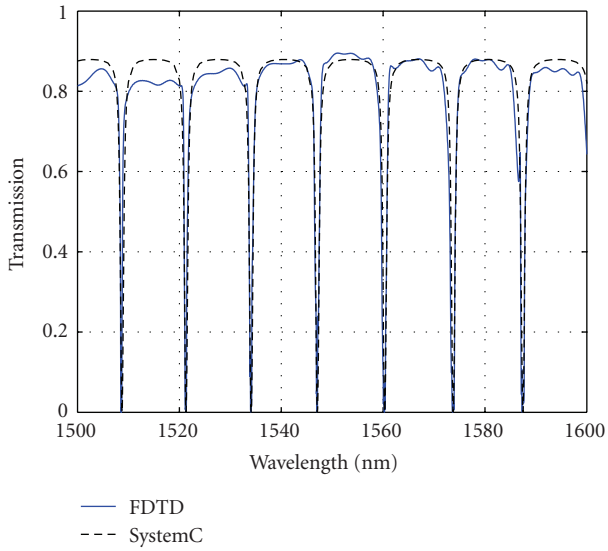

FIGURE 6: Simulated (solid line) and modeled (dashed line) transmission curves for the path linking the I-WEST port with the O-NORTH port of the 4 × 4 optical switch.

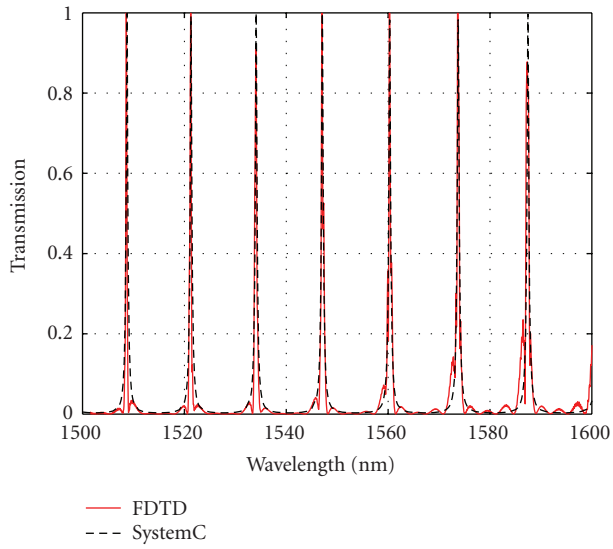

FIGURE 7: Simulated (solid line) and modeled (dashed line) transmission curves for the path linking the I-WEST port with the O-SOUTH port of the 4 × 4 optical switch.

respectively, and n is the number of wavelengths used to compute the response.

The latter PE, on the contrary, can be applied to measure the deviation of the spectral positions and of the peak values, between the resonances obtained by FDTD and SystemC simulations. The expressions allowing the evaluation of these deviations are, respectively,

$$\mathrm{PE}_\lambda = \frac{1}{m}\sum_{i=1}^{m}\left[\left(\frac{\lambda_{\mathrm{SysC}_i} - \lambda_{\mathrm{FDTD}_i}}{\lambda_{\mathrm{FDTD}_i}}\right) * 100\right],$$
$$\mathrm{PE}_V = \frac{1}{m}\sum_{i=1}^{m}\left[\left(\frac{P_{\mathrm{SysC}}(\lambda_i) - P_{\mathrm{FDTD}}(\lambda_i)}{P_{\mathrm{FDTD}}(\lambda_i)}\right) * 100\right]. \quad (11)$$

PE_λ accounts for the error on the spectral position of the peaks and PE_V for the error on the peak values. $\lambda_{\mathrm{SysC}_i}$ and $\lambda_{\mathrm{FDTD}_i}$ are the peak resonances obtained through the analytical model implemented on SystemC and the ones obtained by FDTD. $P_{\mathrm{SysC}}(\lambda_i)$ and $P_{\mathrm{FDTD}}(\lambda_i)$, on the contrary, are the values of the transmission peaks at the wavelength λ_i calculated by means of SystemC and FDTD, respectively; furthermore, m is the number of considered peaks in the band of interest.

The mismatch parameter SE achieves 2.45% when it is calculated in the case of a Drop Path (e.g., from I-WEST to O-SOUTH), whereas in the case of a Through Path (as the one from I-WEST to O-NORTH) the SE value is 1.05%. For

what concerns PE_λ, a 0.0063% stable error for all ports has been calculated; finally, $PE_V = 3.451\%$. This demonstrates the accuracy of the approach based on FDTD + SystemC for the simulation of complex ONoCs.

To further assess the performance of an ONoC, it is fundamental to evaluate the insertion-loss on the critical path (IL_{max}), which is the path between the input and the output presenting the maximum value of losses. This parameter has been calculated in two different cases, with standard elliptical-tapered crossings [22] and with the MMI-based crossings [23], in order to evaluate the impact of the technological choice in the realization of the crossings inside the network. In the first case, IL_{max} is around 2 dB, while it is reduced to 0.56 dB in the second one, thus confirming the better properties of the MMI-based approach to the design of crossings. It is worth noting that the choice between the two possible optimized solutions could also depend on the available space in the physical region around the crossing.

5. SystemC Modelling of a 4×4 Square Root Topology

One of the most important examples of optical network topologies proposed in the literature so far is represented by the 4×4 square root [19]. As illustrated in Figure 8, this interconnection network embeds 16 gateways. Each gateway (G_i) can work as the initiator or the target of the communication and may send and reach optical data from the others; therefore, a parallel communication is possible. This optical architecture is constructed recursively starting from a 2×2 quad, which in turn consists of four 4×4 switches structured in a 2×2 mesh. In this specific case, the four internal rings of each 4×4 switch have different radii with respect to the four external ones. This choice produces two interleaved resonance spectra, allowing the routing from any input of the 4×4 switch to three possible outputs (i.e., routing from West to South if the signal is resonant with the four external rings, routing from West to East if the signal is resonant with the four internal ones, and from West to North if the signal is not resonant with anyone). Notice that every 4×4 switch is connected to another one by utilizing intraquad lines which do not present intersections. A 4×4 square root equips four 2×2 quads (the blocks from A to D in Figure 8) and one central switch (the block indicated by E in the same Figure); interquad express lanes are used for connecting each quad. Connections among them can be realized directly or through the central 2×2 quad. The inter-quad express lanes are affected by additional crossings which our modeling framework takes into account.

Following the compositional approach, even an 8×8 square root topology can be derived by linking four 4×4 square roots. In fact, the recursive design can be exploited to obtain any size of this topology with dimensions equal to any positive integer power of two.

By using the previously obtained SystemC models of the different blocks, as mentioned at point (5) of Section 2, the insertion-loss analysis was accomplished. For brevity, only the case study with injection from gateway G4 is reported. Figure 9 shows the insertion-loss from G4 to all other gateways, without accounting for the interexpress lanes loss-contributions. The paths inside the square root topology are indicated by means of conventional acronyms; the abbreviation GNA stands for communications between the gateway G4 and the North-Eastern gateway of quad A (G1), GED stands for the link between G4 and the South-Eastern gateway of quad D (G14), and so on. In Figure 10, on the contrary, these insertion losses have been taken into account, thus leading to a more accurate evaluation of the overall attenuation of each path and highlighting the importance of the losses for the overall performance of the network. Obviously, by changing from the first to the second scenario, increase of insertion-loss from 0.1 dB up to 2.6 dB is observed.

Our technology-annotated SystemC models clearly enable us to assess the physical properties of optical paths (i.e., a physical design issue), in addition to the traditional functional simulation capability. For the presented structure, the insertion-loss critical path (i.e., the path with the maximum amount of losses) is established from G4 to G14, and it counts 10 dB when each crossing waveguide was designed by using the standard Elliptical Taper. By optimizing every crossing with the MMI-based solution, the insertion-loss is reduced to 4.85 dB.

Once determined the maximum insertion loss of the full network (which corresponds to the worst-case optical path), it is possible to assess the minimum optical power that laser sources should provide to enable correct detection of the optical data stream at the photodetectors with the desired bit error rate (BER) [26].

Hence, by assuming, for example, that

(1) for a given bit error rate (BER) of 10^{-9}, the corresponding detector sensitivity is -20 dBm;

(2) elliptically tapered crossings are used at every intersection;

(3) the data stream is carried over 30 different optical wavelengths.

The laser power injected in the network must be more than 3 mW; this amount of power can be reduced by a factor of about 70% by optimizing each crossing with MMI-based structures, thus achieving 0.92 mW.

With the proposed approach based on the FDTD characterization of the fundamental blocks and a compositional approach in SystemC to form the complex network, the overall simulation times remain very low (fraction of seconds), and investigation of very complex network is certainly possible. In fact, long computation time is only required to characterize through FDTD the basic building blocks of the network, but this must be done only once for each block, when the corresponding *s*-parameters matrix should be determined, and does not need to be repeated each time the corresponding block is replicated inside the network.

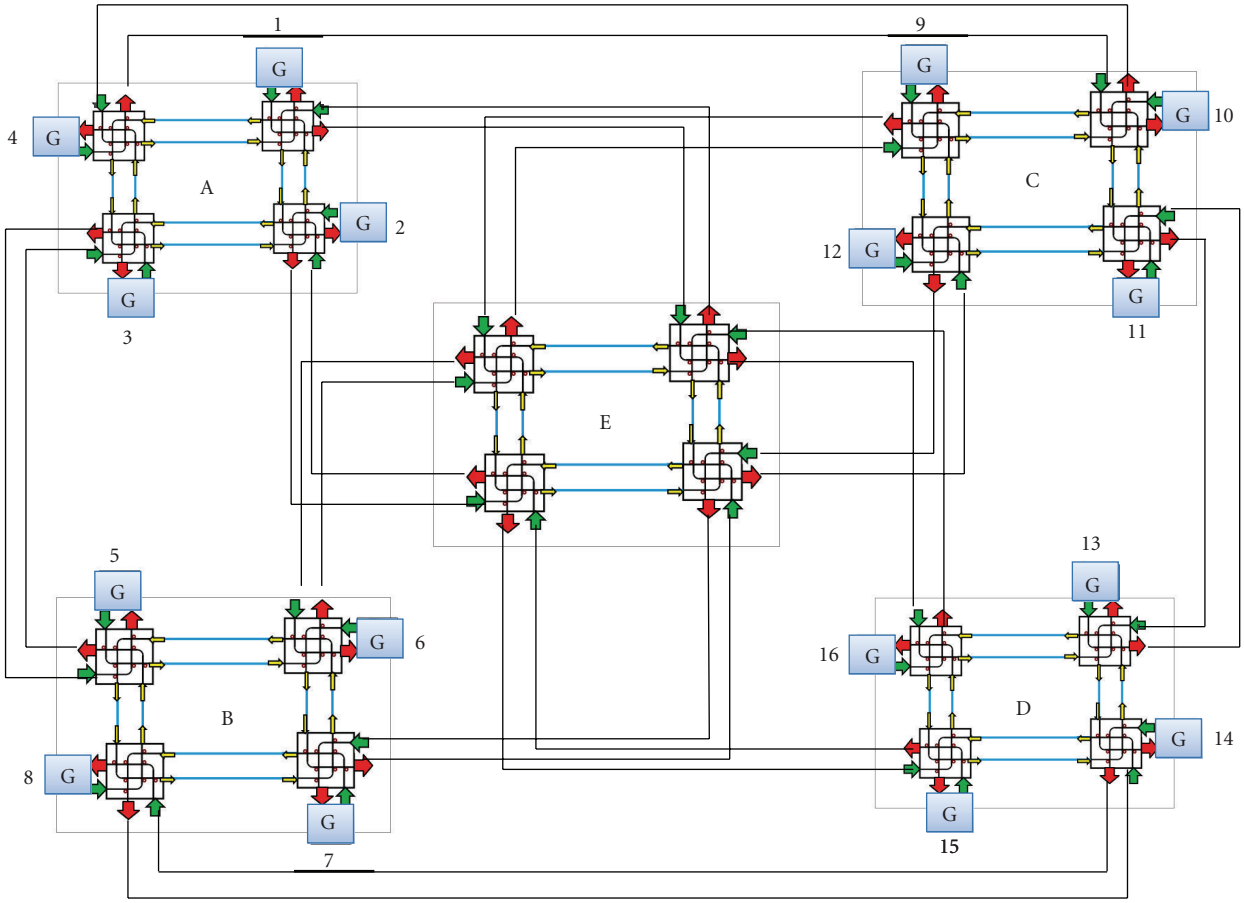

Figure 8: 4 × 4 square root topology.

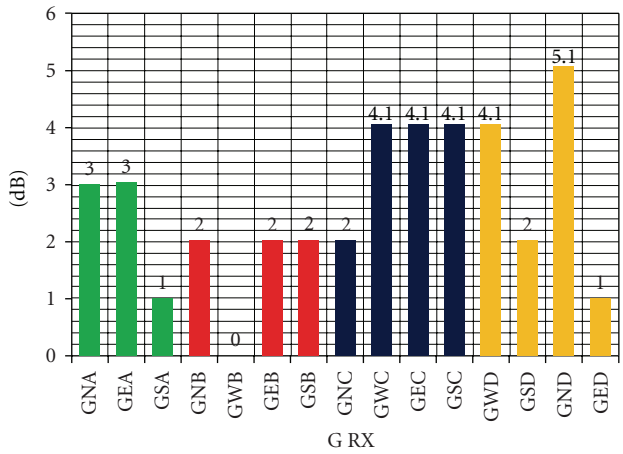

Figure 9: Insertion-loss comparison for the 4 × 4 square root topology of Figure 8, by considering injection from G4 and without accounting for the inter-express lanes loss-contributions. Every intersection is optimized with standard elliptical tapers.

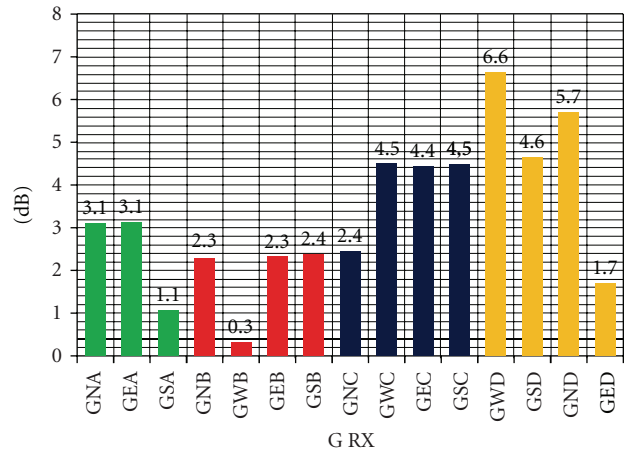

Figure 10: Insertion-loss comparison for the 4 × 4 square root topology of Figure 8, by considering injection from G4 and taking into account the inter-express lanes loss-contributions. Every intersection is optimized with standard elliptical tapers.

6. Conclusions

This work presents a new modelling strategy based on the design-flow FDTD + SystemC in order to explore and simulate optical Network-on-Chip topologies at system level. The procedure relays on the abstraction of the analytical models for the relevant components of an ONoC (rings, waveguide crossings) toward the SystemC environment. The

optical responses of the elementary photonic switching elements are first obtained via 2D-FDTD, then back-annotated in the SystemC modules. The modular and incremental composition of the basic switching elements allows the simulation of arbitrary complex topologies.

A good tradeoff between accuracy in the modelling of the investigated dynamics and simulation times has been demonstrated; furthermore, the error parameters introduced to quantitatively validate the performance of the design flow are largely satisfactory. As a case study, the SystemC modelling of one of the most famous optical network topologies, the 4×4 square root, is proposed, and its insertion-loss assessment for different paths is quantified. Simulation results demonstrate that in the worst case, insertion-loss is 10 dB using standard crossing optimization, while it is reduced at 4.85 dB using MMI-based intersections.

In future works, we aim, firstly, at extending the physical layer library (PLL) and, consequently, the related SystemC photonics library (SPL) in order to build a flexible, reusable, and modular framework for exploring all kinds of ONoCs topologies.

Acknowledgments

This work is supported by the Italian Ministry of the University and Research (MIUR) through PHOTONICA FIRB 2008 and SAPPHIRE PRIN 2009 projects. The authors thank all the members of the PHOTONICA consortium. A. Parini thanks the Programma Operativo FESR 2007–2013 of the Emilia-Romagna Region-Attività I.1.1. for the financial support to his research activity.

References

[1] International Technology Roadmap for Semiconductors (ITRS), http://www.itrs.net/.

[2] D. Bertozzi, A. Jalabert, S. Murali et al., "NoC synthesis flow for customized domain specific multiprocessor systems-on-chip," *IEEE Transactions on Parallel and Distributed Systems*, vol. 16, no. 2, pp. 113–129, 2005.

[3] H. Gu, J. Xu, and Z. Wang, "A novel optical mesh network-on-chip for gigascale systems-on-chip," in *Proceedings of IEEE Asia Pacific Conference on Circuits and Systems (APCCAS '08)*, pp. 1728–1731, December 2008.

[4] A. Shacham, K. Bergman, and L. P. Carloni, "Photonic networks-on-chip for future generations of chip multiprocessors," *IEEE Transactions on Computers*, vol. 57, no. 9, pp. 1246–1260, 2008.

[5] H. Wang, M. Petracca, A. Biberman, B. G. Lee, L. P. Carloni, and K. Bergman, "Nanophotonic optical interconnection network architecture for on-chip and off-chip communications," in *Proceedings of the Conference on Optical Fiber Communication/National Fiber Optic Engineers Conference (OFC/NFOEC '08)*, February 2008.

[6] L. Pavesi and G. Guillot, *Optical Interconnects, The Silicon Approach*, Springer, Berlin, Germany, 2006.

[7] C. Gunn, "CMOS Photonics for High-Speed Interconnects," *IEEE Micro*, vol. 26, no. 2, p. 5866, 2006.

[8] Y. Halioua, A. Bazin, P. Monnier et al., "Hybrid III-V semiconductor/silicon nanolaser," *Optics Express*, vol. 19, no. 10, pp. 9221–9231, 2011.

[9] L. Ottaviano, E. Semenova, M. Schubert et al., "High-speed photodetectors in a photonic crystal platform," in *CLEO: Science and Innovations, Detectors & Sources (CM1A)*, San Jose, Calif, USA, May 2012.

[10] C. Husko, S. Combrié, Q. Vy Tran, F. Raineri, C. W. Wong, and A. De Rossi, "Non-trivial scaling of self-phase modulation and three-photon absorption in III-V photonic crystal waveguides," *Optics Express*, vol. 17, no. 25, pp. 22442–22451, 2009.

[11] N. Sherwood-Droz, H. Wang, L. Chen et al., "Optical 4×4 hitless silicon router for optical Networks-on-Chip (NoC)," *Optics Express*, vol. 16, no. 20, pp. 15915–15922, 2008.

[12] X. Yin, H. Gu, H. Ju, and L. Jia, "An electro optical honeycomb networks-on-chip based on a new nonblocking switch," in *Proceedings of the 23rd International Technical Conference on Circuits/Systems, Computers and Communications*, 2008.

[13] X. Tan, M. Yang, L. Zhang, Y. Jiang, and J. Yang, "On a scalable, non-blocking optical router for photonic networks-on-chip designs," in *Proceedings of the Photonics and Optoelectronics (SOPO '11)*, May 2011.

[14] I. O'Connor, M. Brière, E. Drouard et al., "Towards reconfigurable optical networks on chip," in *Proceedings of the Reconfigurable Communication-centric Systems-on-Chip workshop (ReCoSoC '05)*, pp. 121–128, 2005.

[15] J. Chan, G. Hendry, A. Biberman, K. Bergman, and L. P. Carloni, "PhoenixSim: a simulator for physical-layer analysis of chip-scale photonic interconnection networks," in *Proceedings of the Design, Automation and Test in Europe Conference and Exhibition (DATE '10)*, pp. 691–696, March 2010.

[16] E. Drouard, M. Briere, F. Mieyeville, I. O'Connor, X. Letartre, and F. Gaffiot, "Optical Network on chip Multi-Domain modelling using SystemC," in *Proceedings of the Forum on Specification and Design Languages*, pp. 123–135, 2004.

[17] M. Briere, E. Drouard, F. Mieyeville et al., "Heterogeneous modelling of an optical network-on-chip with systemC," in *Proceedings of the IEEE International Workshop on Rapid System Prototyping*, pp. 10–16, 2005.

[18] K. S. Yee, "Numerical solution of initial boundary value problems involving Maxwell's equations in isotropic media," *IEEE Transactions on Antennas and Propagation*, vol. 14, pp. 302–307, 1966.

[19] J. Chan, G. Hendry, A. Biberman, and K. Bergman, "Architectural exploration of chip-scale photonic interconnection network designs using physical-layer analysis," *IEEE Journal of Lightwave Technology*, vol. 28, no. 9, Article ID 5423995, pp. 1305–1315, 2010.

[20] J. Van Campenhout, W. M. J. Green, and Y. A. Vlasov, "Design of a digital, ultra-broadband electro-optic switch for reconfigurable optical networks-on-chip," *Optics Express*, vol. 17, no. 26, pp. 23793–23808, 2009.

[21] O. Schwelb, "Transmission, group delay, and dispersion in single-ring optical resonators and add/drop filters—a tutorial overview," *Journal of Lightwave Technology*, vol. 22, no. 5, pp. 1380–1394, 2004.

[22] N. Sherwood-Droz, H. Wang, L. Chen et al., "Optical 4×4 hitless silicon router for optical Networks-on-Chip (NoC)," *Optics Express*, vol. 16, no. 20, pp. 15915–15922, 2008.

[23] H. Chen and A. W. Poon, "Low-loss multimode-interference-based crossings for silicon wire waveguides," *IEEE Photonics Technology Letters*, vol. 18, no. 21, pp. 2260–2262, 2006.

[24] G. R. Simpson, "A generalized n-port cascade connection," *IEEE MTT-S International Microwave Symposium Digest*, vol. 81, no. 1, pp. 507–509, 1981.

[25] J. Chan, A. Biberman, B. G. Lee, and K. Bergman, "Insertion loss analysis in a photonic interconnection network for on-chip and off-chip communications," in *Proceedings of the 21st Annual Meeting of the IEEE Lasers and Electro-Optics Society (LEOS '08)*, pp. 300–301, November 2008.

[26] G. Agrawal, *Nonlinear Fiber Optics, (Optics and Photonics)*, Academic Press, 3rd edition, 2001.